ENGULF: Coastal land subsidENce in the GULF of Guinea

The case of Dakar and Cape Verde Peninsula (Senegal): Vertical land motion, its relations to hydrogeology and land-use and implications for relative sea-level rise and flood exposure

---

Final report

to the Agence Française de Développement

on the research conducted in the ENGULF Program

–

compiled by

Cheikh Tidiane **Wade**[1], Roberta **Boní**[2], Katharina **Seeger**[3], Fatou **Diop Ngom**[1], Oluwaseyi **Dasho**[4], Philip S. J. **Minderhoud**[3], Marie-Noëlle **Woillez**[5] and Pietro **Teatini**[6]

Authors' affiliation: [1] Cheikh Anta Diop University (Ghana) ; [2] University of Pavia (Italy); [3] University of Wageningen (the Netherlands); [4] Virginia Tech (USA); [5] French Agency for Development (France); [6] University of Padua (Italy)

Padova, 2025

Contents

1 Introduction

With its low elevation and dense population, the coastline along the Gulf of Guinea faces a high exposure to coastal erosion and sea-level rise. While coastal erosion is comparably well understood (e.g., Alves et al., 2020; Dada et al., 2021; Almar et al., 2023; Ankrah et al., 2023; Dada et al., 2024), the long-term hazard of sea-level rise is not. To assess this hazard and consequently exposure and vulnerability, the effects of both global, climate-induced sea-level rise and vertical land movement in form of coastal land subsidence, resulting in relative sea-level rise, need to be considered. Along the Gulf of Guinea coast, knowledge about relative sea-level rise is scarce and coastal subsidence, its spatio-temporal pattern and its impact is a huge unknown. The ENGULF project addresses these gaps by providing up-to-date quantifications of present coastal land subsidence from Interferometric Synthetic Aperture Radar (InSAR) measurements and integrating them into first, tentative assessments of potential future relative sea-level rise impact using latest available elevation data corrected to continuous local mean sea level.

The Cape Verde Peninsula with Dakar City (Senegal) constitutes one focus area under the umbrella of the ENGULF program. Previous works documented coastal subsidence in the port area of Dakar (Le Cozannet et al., 2015), yet a regional investigation including physical and anthropogenic drivers as well as implications on relative sea-level rise and flood exposure is missing. Within the ENGULF program, a state of the art on the geological, hydrogeological and land-use setting was established and used to explain new estimates of vertical land motion derived from Interferometric Synthetic Aperture Radar (InSAR) processed under the umbrella of ENGULF. This report summarises the research activities conducted and concludes with an outlook on the implications for relative sea-level rise and flood exposure of this region.

2 Setting

2.1 Geology

The Cape Verde Peninsula is part of the broader Senegal-Mauritania sedimentary basin. It is a structurally complex area characterised by a monoclinal westward dip of sedimentary layers and a system of sub-meridian faults forming structural compartments such as the Dakar Horst and the Rufisque Graben (Figs. 1 and 2). In addition, volcanic intrusions (dated to the Neogene) disrupt the stratigraphic continuity and introduce harder materials into otherwise soft sedimentary series.

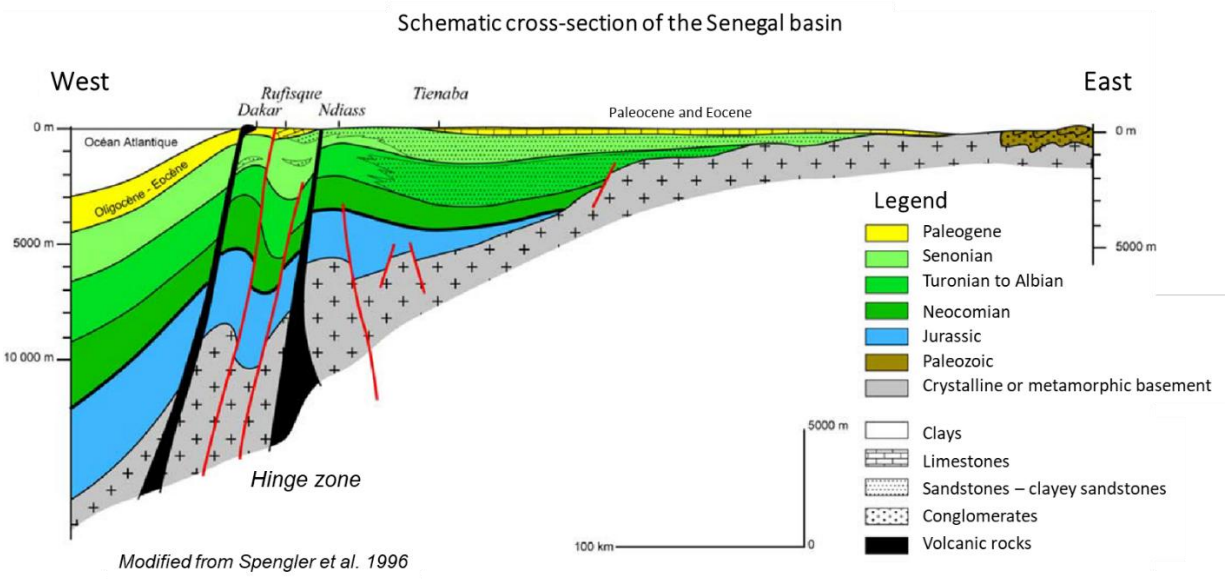

Figure 1 | West-East cross-section of the Senegal Basin (south of Dakar - Korkol ferlo) (Barusseau et al. (2009), modified from Spengler et al., 1966).

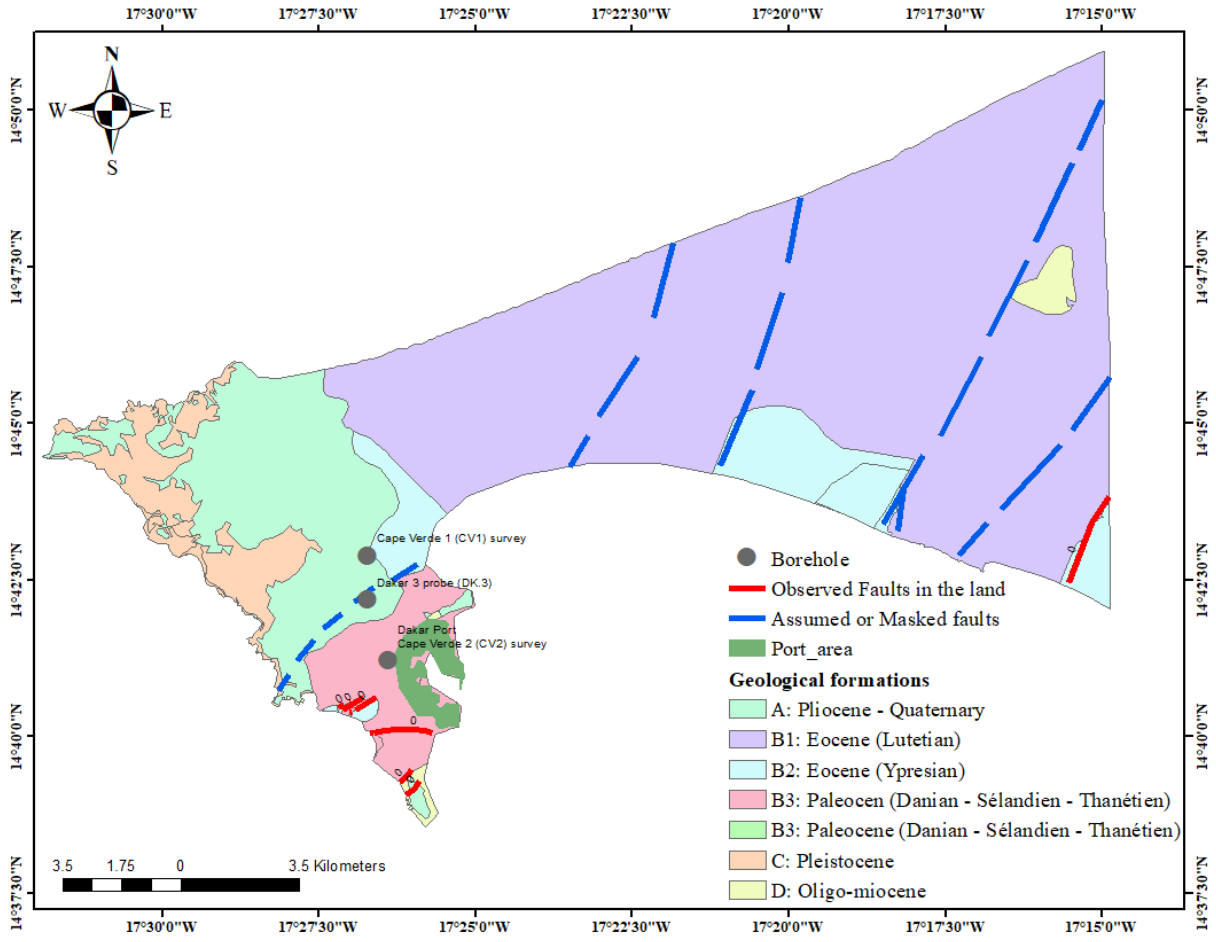

Figure 2 | Geological surface map of the Cape Verde Peninsula.

These structural features contribute to differential compaction and vertical displacements that may induce mechanical stress on aquifer systems and urban surfaces. Additionally, marine regression and transgression phases have shaped the sedimentary infill, depositing alternating marls, clays, and sands. This heterogeneity plays a crucial role in the response of the subsurface to stress and infiltration.

The lithostratigraphic analysis of the three boreholes (DK3, CV1, and CV2, see Fig.2) provides a detailed understanding of subsurface stratification and vertical continuity. The geological logs were interpreted based on lithological descriptions and chronostratigraphic units, allowing the identification of fifteen distinct formations ranging from Quaternary deposits to Lower Cretaceous sequences. This classification supports the assessment of natural subsurface deformation potential under varying hydrostatic and geochemical conditions (see Fig. 3). The surveys were conducted in the Dakar Port Zone (DK3) and the inland sector of the Cape Verde Peninsula (CV1 and CV2), and the resulting profiles show strong vertical stratigraphic coherence across the study area.

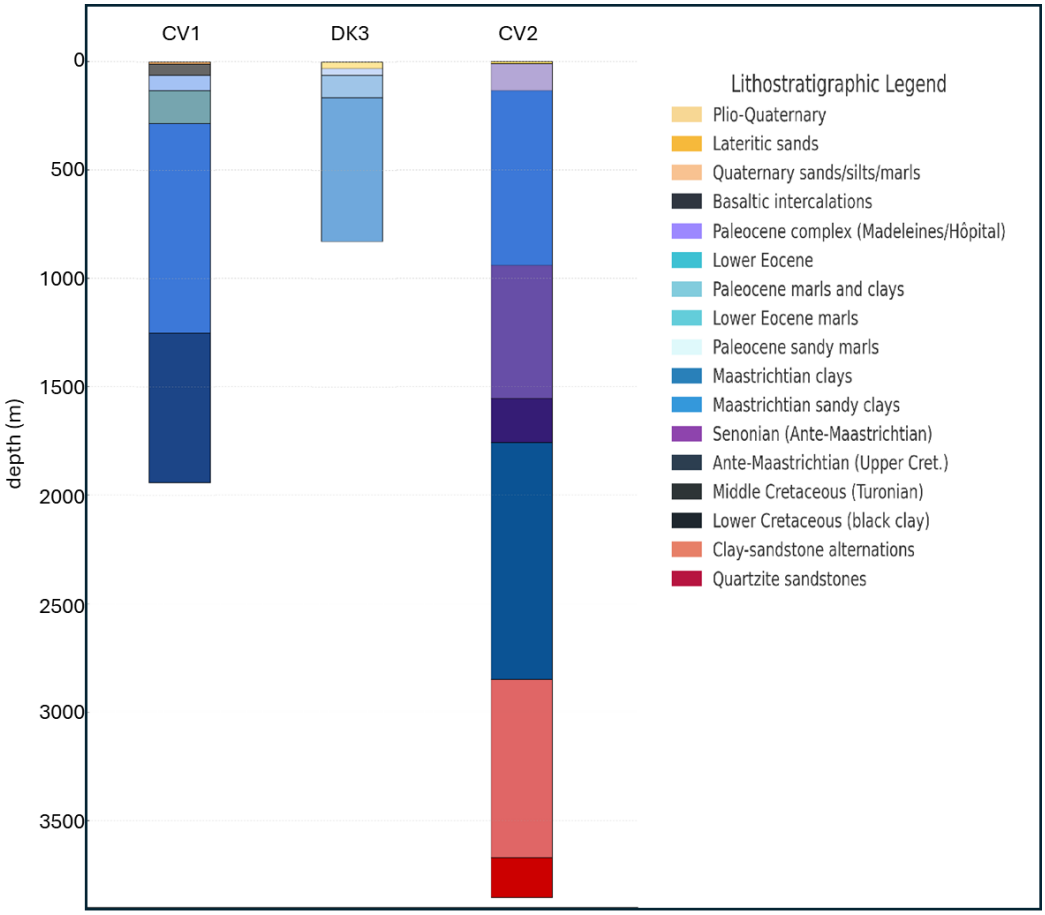

Figure 3 | Lithostratigraphic profiles of boreholes DK3, CV1, and CV2 showing vertical continuity and geological formations from Quaternary to Lower Cretaceous units. The colour legend is oriented by depth.

The uppermost unit (Unit I) corresponds to the Quaternary sands and silts, with an average thickness of 6 to 10 meters. These sediments, deposited through coastal and aeolian processes, exhibit high permeability and relatively loose structure, which makes them sensitive to mechanical disturbance. However, due to their limited depth, they are typically unsaturated or variably saturated, depending on seasonal recharge and proximity to the water table. Beneath lies the Palaeocene to Maastrichtian unit (Unit II), dominated by marls, soft limestones, and calcareous clays. This layer is prone to dissolution and mechanical weakening due to its low cohesion and susceptibility to chemical weathering, especially under saturated conditions. The presence of water within this unit reduces shear strength and favors compaction, contributing to potential settlement. The Upper Cretaceous unit (Unit III) is composed of plastic clays and fossiliferous marls. Given its depth and clayey texture, this layer is assumed to be permanently saturated, limiting moisture fluctuations. However, its high capillary activity and plasticity make it susceptible to long-term vertical shrinkage and secondary consolidation, which may contribute to differential settlements under load. The Middle Cretaceous unit (Unit IV), characterized by dark marls and blue clays, behaves as a semi-confined aquitard. In cases where this unit is punctured by faults or boreholes, it may induce a release of confined pressure, influencing the overlying aquifers and potentially destabilizing the upper layers. At greater depth, the Volcanic Intercalations (Unit V) composed of basaltic tuffs, ash, and hard clays, act as a hydraulic barrier. Their mechanical contrast with surrounding soft layers may enhance vertical stress differentials and favor localized subsidence in overlying compressible units.

Overall, this lithostratigraphy suggests that the region is inherently prone to deformation, particularly under fluctuating hydrostatic loads and progressive chemical alteration. The combination of low-permeability clays, soluble carbonates, and confined pressures highlights a complex geomechanical setting requiring careful monitoring in urban development projects.

2.2 Hydrogeology

The hydrogeological regime of the Cape Verde Peninsula comprises two main aquifer systems (Fig.4):

- A shallow Quaternary aquifer, made up of unconsolidated sandy and aeolian deposits, with groundwater levels observed at various depths depending on local topography and recharge (British Geological Survey, 2023).

- A deeper Maastrichtian aquifer, consisting of calcareous sandstones from the Upper Cretaceous, with a saturated thickness typically around 250 m, which serves as a primary regional water-bearing unit (Kane et al., 2012; Faye et al., 2019).

Other hydrostratigraphic units, such as infrabasalitic sands and palaeovalley deposits, have been documented regionally, but precise depth data remain unavailable in accessible scientific literature.

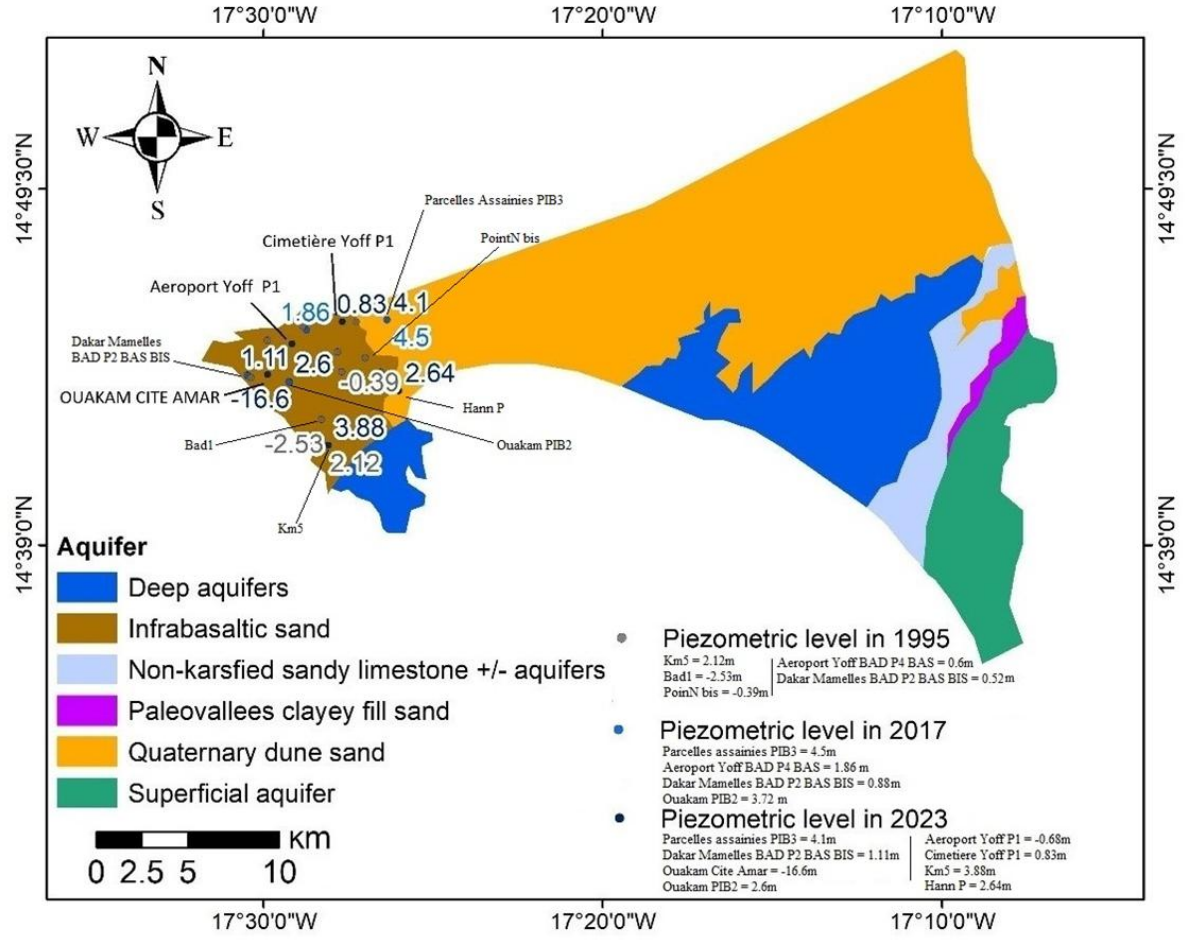

Figure 4 | Hydrogeological map of Dakar showing groundwater level measurements (in m above mean sea level) from observation wells in 1995, 2017 and 2023. Each point corresponds to a labelled well (e.g., Yoff P1, Ouakam Cité Amar) used to assess piezometric evolution.

Among these, the Quaternary dune sands constitute unconfined aquifers with high permeability, allowing for rapid recharge and making them particularly susceptible to salinisation (see also Section 2.1 and Fig. 3). The infrabasalts, on the other hand, show moderate transmissivity and behave as semi-confined aquifers, with relatively good recharge potential under natural conditions. In contrast, the deep aquifers are confined systems, typically located between low-permeability layers, and thus remain under natural pressure. Excessive groundwater extraction (overpumping) from these confined aquifers can reduce

pore water pressure, causing compaction of the aquifer matrix. This process is often irreversible and may result in land subsidence, particularly in coastal or heavily urbanised areas (see also Section 2.1).

2.3 Land use

Information on land use/land cover in the Cape Verde Peninsula was obtained by utilising high-resolution Sentinel-2 imagery (spatial resolution: 10 m) along with global Esri land cover data for the years of 2018 and 2022 (Esri and Impact Observatory, 2005). In 2018, most of the land constituted built-up areas (ca. 45%, corresponding to about 244.94 km²) and rangelands (ca. 40%, corresponding to ca. 219.39 km²) (Fig. 5a).

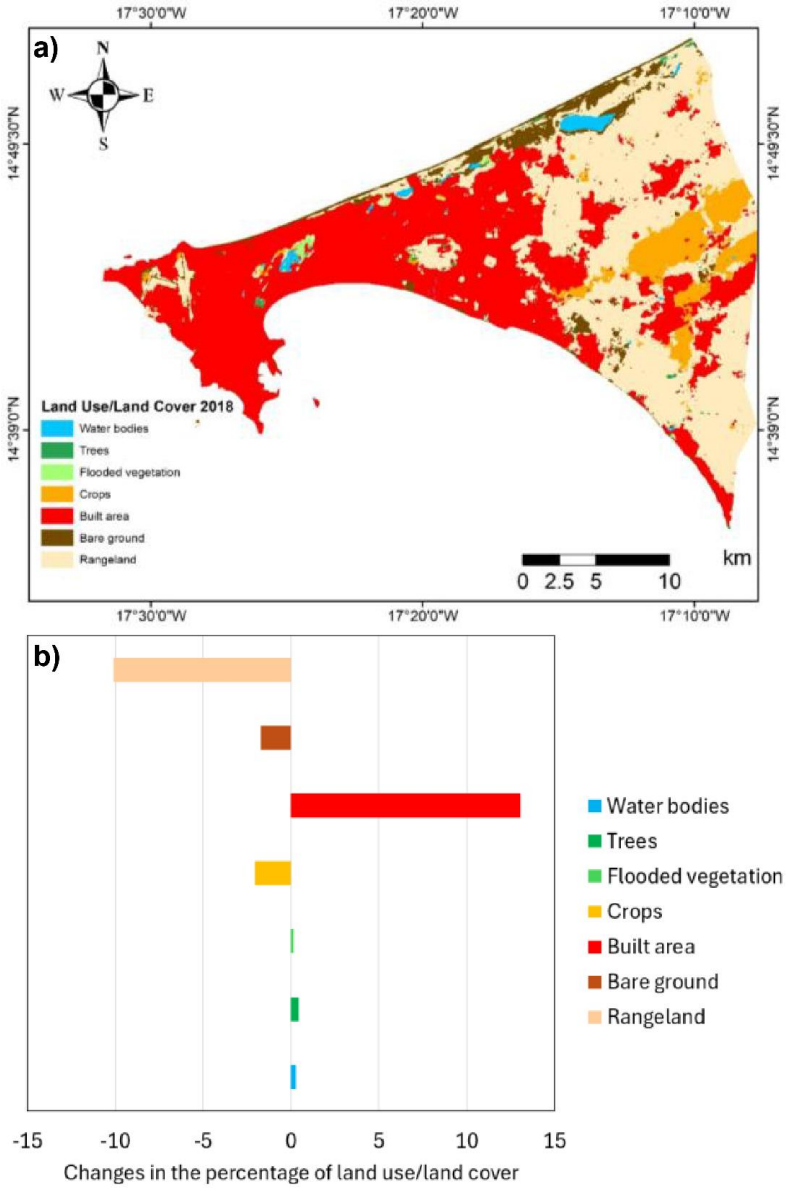

Figure 5 | (a) Land Use/Land Cover of Cape Verde Peninsula in 2018 and (b) land use/land cover change in the same area between 2018 and 2022 (Esri and Impact Observatory, 2025).

Crops made up about 7% of the area, while bare ground constituted around 5%. Minor land cover classes such as water bodies, trees, and flooded vegetation each occupied less than 1% of the total area (Fig. 5a). From 2018 to 2022, the built-up area has expanded and increased by 13%, mainly at cost of rangeland which decreases by 10% (Fig. 5b). Similarly, the coverage of cropland and bare ground decreases while a slight increase in flooded vegetation and tree cover is noticed (Fig. 5b).

3 Hydrochemistry and Hydromechanics

3.1 Hydrochemical and hydromechanical investigations

Hydrochemical analyses performed on groundwater samples collected in 2023 reveal a predominant presence of calcium, bicarbonate, and magnesium ions, as shown in the updated Piper diagram (Fig. 6). Most samples fall within the Ca–Mg–HCO_3 hydrochemical facies, indicating a fresh groundwater type typically associated with carbonate dissolution and silicate weathering. However, slight deviations toward the SO_4 and Cl fields can be observed, particularly in coastal zones, suggesting localized influences of anthropogenic activities and potential salinization.

These water types are generally characterized by low mineralization, consistent with shallow aquifers, but may evolve under conditions of mixing or recharge from marine or polluted sources. The presence of magnesium and chloride in specific locations supports the hypothesis of ionic exchange processes and possibly marine intrusion, which could influence both the chemical reactivity and geotechnical behavior of the sediment matrix (e.g., clay deflocculation, pore pressure variation).

Therefore, the updated Piper diagram provides a clearer classification of groundwater types, helping to identify zones of potential hydrogeochemical vulnerability and supporting the interpretation of hydro-mechanical risks in the study area.

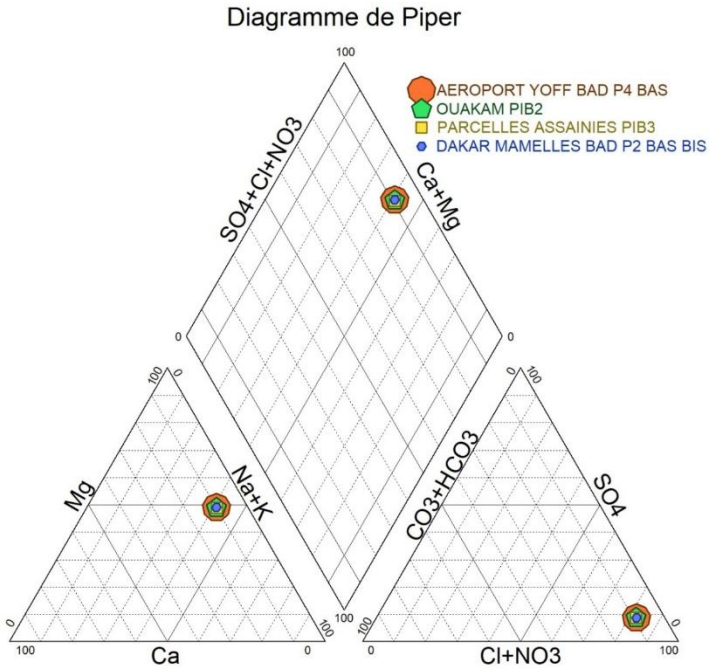

Figure 6 | Piper diagram representing the chemical composition of groundwater (2017), plotted from ionic concentrations in mg/L.

To gain insights into the groundwater dynamics of the peninsula, piezometric measurements collected over a 28-year period (1995–2023) were analysed. These measurements originate from a consistent set of observation wells distributed across the Cape Verde Peninsula. The piezometric levels were calculated using the formula:

Piezometric level = Ground surface elevation – Water depth,

meaning that all values are referenced to mean sea level (MSL).

As such, the results reflect the actual hydraulic head elevations, enabling valid spatial and temporal comparisons across the study area. In 1995, the groundwater levels ranged from -7.7 m to +2.1 m above sea level. In 2017, they ranged from -4.5 m to +0.8 m, and in 2023, the levels varied from -16 m to +4 m, with some sites showing a significant drawdown. These variations reveal a decline in groundwater levels in some areas over time, possibly related to increasing extraction and/or reduced recharge. Table 1 provides the regional averages and variability (standard deviation) of piezometric levels for each year, while Fig. 4 presents the spatial distribution of the groundwater levels records, allowing a visual comparison across the peninsula as of 1995, 2017, and 2023.

Year	Mean (m)	Standard deviation (m)
1995	1.1	0.84
2017	2.7	1.66
2023	2.9	1.38

Table 1 | Average piezometric levels obtained from key sites Km5, Dakar Mamelles BAD P2 BAS BIS, Aéroport Yoff P1, Parcelles Assainies PIB3, and Ouakam PIB2 in the Cape Verde Peninsula. Locations of the piezometric measurements are provided in Fig. 4.

Groundwater level variations in the Cape Verde Peninsula between 1995 and 2023 reveal a spatially heterogeneous behavior. While the overall trend could reflect a slight regional rise, site-specific trajectories reflect contrasting hydrogeological dynamics. At the Km5 Seydou Nourou site, for instance, the water table increased from 2.1 m in 1995 to 3.9 m in 2023, while the Ouakam PIB2 site recorded a decline, from 3.7 m in 2017 to 2.6 m in 2023. Differently, Parcelles Assainies PIB3 remained relatively stable (from 4.5 m to 4.1 m), highlighting the spatial complexity of piezometric responses across the peninsula.

To evaluate the statistical significance of these temporal variations, two-sample t-tests were applied. The mean difference between 1995 and 2017 was -1.6 m ($p = 0.20$), while that between 2017 and 2023 was -0.2 m ($p = 0.87$). Both p-values exceed the 0.05 threshold, indicating that the observed changes are not statistically significant at the regional scale. These results confirm that, despite visually noticeable fluctuations at certain locations, the overall piezometric regime has remained relatively stable from a statistical perspective. Moreover, it must be highlighted that the observed changes in groundwater levels could also merely reflect natural interannual or seasonal variability. The lack of continuous records hinders the ability to conclusively assess the existence of significant trends and, if any, the relative contribution of natural versus anthropogenic factors.

From a hydrogeological viewpoint, the most pronounced declines are concentrated in the northwestern and western sectors of the peninsula, particularly Ouakam PIB2 and areas of Hann, where aquifers are mainly composed of infra-basalitic sands. These permeable formations are more prone to rapid drainage and exhibit heightened sensitivity to abstraction-induced depressurization. In contrast, stable or rising levels are observed in fractured volcanic zones such as Km5 and Dakar Mamelles, where recharge may be more efficient, and pressure losses more limited due to the fractured nature of the host rock.

These observations underscore the critical influence of lithological context and anthropogenic pressures in shaping local piezometric trajectories. Even in the absence of a statistically significant trend at the scale of the peninsula, localized drawdowns in sandy or compressible

units may generate important hydro-mechanical responses. In particular, areas like Ouakam and Hann, where infra-basalitic sands are overlain by dense urban infrastructure, could be vulnerable to progressive land subsidence, especially under conditions of sustained pressure decline and low recharge rates.

3.2 Hydro-mechanical Implications and Subsurface Deformation Potential

The detected spatial heterogeneity in groundwater levels remains a central variable in subsidence modelling. Localized declines, even when not statistically significant across the region, may induce critical stress redistributions in the subsurface, potentially leading to shear deformation, vertical displacement, and differential compaction. Such processes, if unmonitored, could compromise surface infrastructure and exacerbate risks in urbanized zones.

Although the spatio-temporal trends observed between 1995 and 2023 do not indicate significant piezometric decline at the macro scale, specific zones such as Ouakam PIB2 show enough drawdown to warrant hydro-mechanical concern. These localized variations suggest that the mechanical response of the subsurface may vary significantly across lithological boundaries, with potential consequences for structural stability.

Several coupled processes must be taken into account in this context:

1. Consolidation of compressible sediments (e.g., clays, marls) following long-term pressure loss;
2. Increase of effective stress in exploited aquifers, resulting in irreversible compaction;
3. Increase in effective vertical stress under anthropogenic loads (urban, industrial), particularly in high-density sectors such as Hann and Ouakam;
4. Reactivation of pre-existing fault systems under conditions of hydrostatic disequilibrium, especially in geologically sensitive areas.

These interrelated mechanisms highlight the importance of adopting an integrated approach that combines hydrogeological monitoring, geological mapping, and anthropogenic load assessment to fully understand the vertical land motion currently affecting the Dakar Peninsula. A robust interpretation of groundwater behavior must move beyond statistical trends to include litho-structural and socio-economic parameters likely to influence aquifer dynamics and surface deformation.

3.3 Implications of geology, hydrogeology and hydromechanics for understanding vertical land motion in the Cape Verde Peninsula

By combining geological, hydrogeological and hydrochemical insights, five key mechanisms have been identified as contributors to the vertical land motion observed across the Cape Verde Peninsula. While these processes may interact in complex ways, their respective impacts vary according to lithological setting, aquifer behavior, and anthropogenic pressures. Based on the magnitude of observed deformation and spatial correlation with known drivers, the following mechanisms are presented in order of decreasing importance.

3.2.1 Groundwater overexploitation and depressurization of confined aquifers

Widespread groundwater abstraction, especially for municipal and industrial use, has caused a marked decrease in piezometric levels in certain sectors, notably Ouakam and Hann. This depressurization affects confined aquifers (e.g. infra-basalitic, Maastrichtian), reducing pore pressure and increasing effective stress. The mechanical response includes compaction of saturated layers, which is largely irreversible and leads to permanent land subsidence. This mechanism aligns with areas showing the highest vertical displacement on InSAR maps. Notice that the subsidence rates are relatively small (at least compared to other coastal zones worldwide) suggesting a relative stiff subsurface system at large depth.

3.2.2 Lithological compressibility and consolidation of soft sediments

The presence of compressible layers, such as Palaeocene marls, Cretaceous clays and altered calcareous formations, amplifies subsidence where hydraulic equilibrium is disturbed. These units exhibit high porosity and low shear strength, making them vulnerable to consolidation under stress. When pressure drops due to pumping or chemical alteration, these sediments compact, particularly beneath built-up areas.

3.2.3 Anthropogenic loading from urban development and infrastructure

The rapid expansion of urban areas (e.g., Dakar Plateau, Hann, Ouakam) imposes increasing static loads on subsurface formations. Where these loads coincide with soft lithologies and pressure-depleted aquifers, vertical displacement is exacerbated. The superimposition of buildings, roads, and port installations adds to the risk, particularly in low-lying districts.

3.2.4 Fault reactivation and structural instability

The Cape Verde Peninsula is crossed by NE–SW trending faults that segment the sedimentary basin. While regional tectonic activity is moderate, local InSAR anomalies suggest vertical

offsets along fault lines. Where faults intersect saturated or mechanically weak formations, differential movements may be triggered or enhanced by hydrostatic disequilibrium. These zones may act as focal points for shear deformation and localized subsidence.

3.2.5 Marine intrusion and hydrochemical weakening

Coastal sectors exposed to marine intrusion, such as Hann and Yoff, display elevated concentrations of Na^+ and Cl^- in groundwater. Sodium replaces calcium and magnesium in clays through cation exchange, weakening structural bonds in fine-grained sediments. This hydrochemical alteration promotes dispersion and reduces shear strength, increasing the potential for vertical settlement over time.

Summary and Implications

The above hierarchy highlights groundwater exploitation and lithological sensitivity as the primary drivers of land deformation, followed by surface loading, fault-related subsidence, and salinization-induced weakening. This revised ordering reflects the spatial match between InSAR-measured displacements and zones affected by aquifer depressurization and soft sediment deformation. Future monitoring should prioritize multi-risk zones, especially where geological and anthropogenic drivers converge, to mitigate long-term ground instability in Dakar's coastal belt.

4 Vertical land motion in Cape Verde Peninsula and Dakar: New insights and comparison with existing information

To unravel spatio-temporal patterns of vertical land motion in the study area, a wavelet-based multi-temporal Differential InSAR (DInSAR) algorithm was applied to open and freely available Sentinel-1 SAR data (Shirzaei and Bürgmann, 2012; Shirzaei, 2013; Shirzaei et al., 2019; Lee and Shirzaei, 2023). Latest available algorithms for pair and pixel selection as well as atmospheric error correction were used (Lee and Shirzaei, 2023). Assuming vertical movement to be the main displacement component, satellite unit vectors (Hanssen, 2001) were used to project line-of-sight (LOS) in the vertical direction. The investigated Sentinel-1 SLC imagery (IW mode; 10 m spatial resolution) included data from 2018 to 2023 and covered an area of 542.50 km^2, spanning over five administrative districts. The analysis revealed that the Cape Verde Peninsula is experiencing vertical land motion rates ranging from -13.5 mm/yr to 17.8 mm/yr, with a mean of approximately -1.0 mm/yr and a standard deviation of 1.9 mm/yr. Fig. 7 shows the InSAR velocity map that is referenced to the IGS14 global reference frame and assumed to represent local vertical land motion. 25 % of the measuring points show values

higher than 2 mm/yr and lower than -2 mm/yr. Negative vertical land motion (assumed to represent land subsidence) particularly occurs in the northwestern part and the southern part of the peninsula, where Dakar City is located (Fig. 7). The InSAR dataset shows values higher than 2 mm/yr, with local positive VLM in the inland part of the study area. These anomalies, whether real or unreal, will be further investigated; however, their interpretation is beyond the scope of this study, which focuses on land subsidence in the coastal area of Dakar.

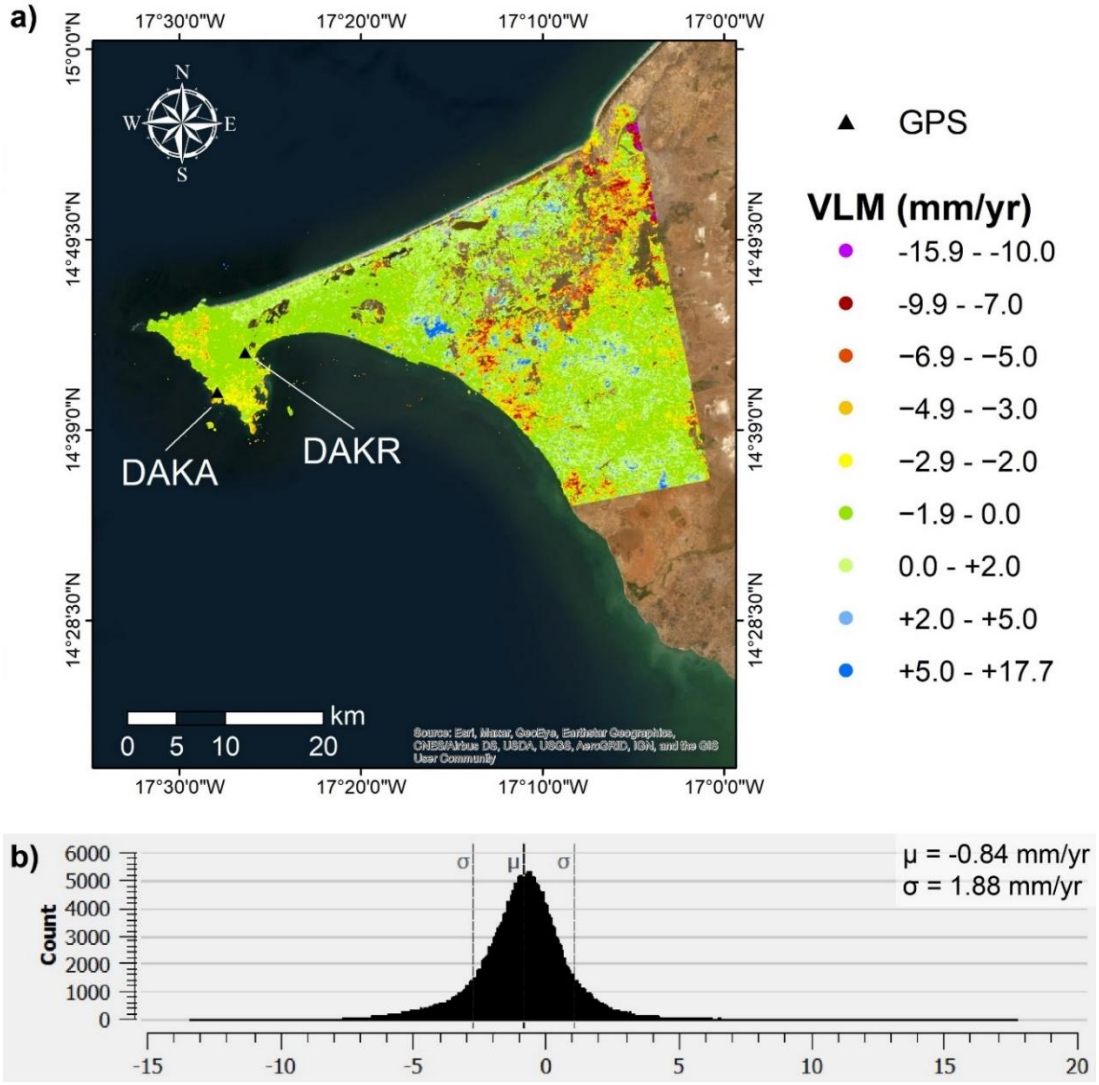

Figure 7 | Average annual vertical land motion (VLM) in Cape Verde Peninsula estimated between 2018 and 2023. (a) Spatial pattern of VLM with red points indicating higher land subsidence values while blue ones indicate uplift. (b) Frequency distribution of VLM (mm/yr) with mean VLM and standard deviation. The displacements refer to the IGS14 global reference frame.

To investigate the accuracy and reliability of the InSAR-derived estimates of vertical land motion calls for a cross-check with precise and accurate GNSS data. However, the two GPS stations (i.e., DAKA and DAKR) located in the study area are decommissioned. These instruments provide GNSS records from 2002 to 2007 and from 2012 to 2021 (Fig. 8). They

were analysed at the Jet Propulsion Laboratory, California Institute of Technology under contract with the National Aeronautics and Space Administration. While a cross-comparison between the InSAR-based and GNSS-based time series cannot be performed due to the missing overlap of investigation periods, the GNSS data at least confirm low subsidence rates for these locations.

Indeed, during the period 2002–2007, the DAKA station recorded a vertical velocity of -0.7 ± 2.9 mm/yr, while the InSAR data estimated within a 50 m buffer zone from the GNSS station shows a VLM value of -2.3 ± 0.5 mm/yr for the period 2018–2023. At the DAKR station, a vertical velocity of -0.4 ± 0.4 mm/yr was observed in the period 2012–2021, while the InSAR data estimated a VLM value of -1.5 ± 0.5 mm/yr within a 50 m buffer zone from the GNS station for the period 2018–2023.

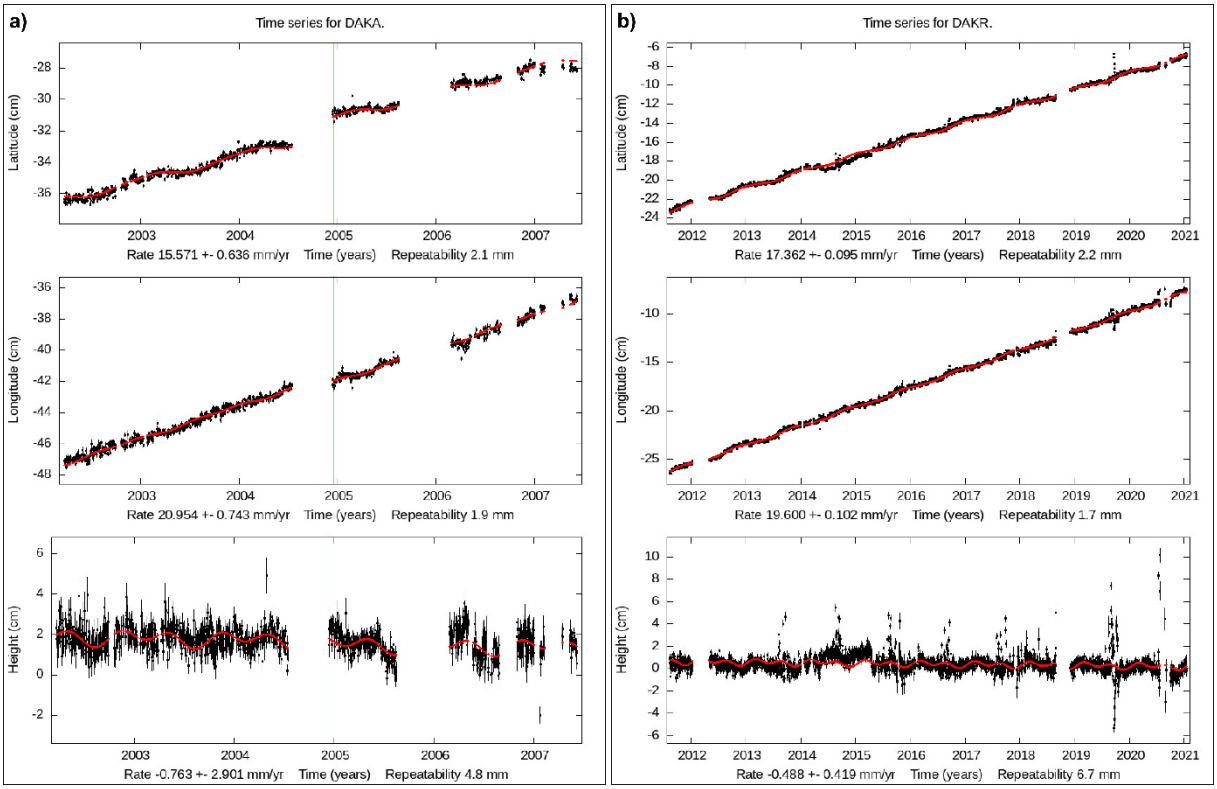

Figure 8 | Displacement time series for the GNSS stations DAKA (a) and DAKR (b), with the average VLM that amounts to -0.8 mm/year and -0.4 mm/year, respectively. The location of the GNSS stations is provided in fig. 7.

Previous works include the studies of Le Cozannet et al. (2015) who investigated vertical land motion in Dakar by using ERS and Envisat InSAR data for the period of 1992 to 2010. The authors identified a unique significant subsidence in the harbour of Dakar, probably due to embankment works in the northern part of the harbour. For the observation of this study, i.e.

from 2018 to 2023, average values for the harbour were -2 mm/yr, in agreement with Le Cozannet et al. (2015), while highest subsidence rated reached -5 mm/yr (Fig. 7).

5 Unravelling drivers of vertical land motion

Despite insufficient hydrogeological, geomechanical, and piezometric data to establish clear cause-effect relationships, we attempted to link measured VLM with in-situ characterization. The results should be interpreted cautiously.

5.1 Relations between vertical land motion and geology

The comparison between estimates of VLM and the geological units of the substratum (Fig. 2; Barusseau et al., 2009; Roger et al., 2009) was performed by extracting the maximum, minimum, average, median, 1st and 3rd quartile values for each age of the geological map units (i.e. geological formations at the surface). The peak of the average subsidence rates was found for the Pliocene-Quaternary formations (i.e., -2.8 mm/yr), and a roughly decreasing trend of the median values is evident towards the older geological formations (i.e., Eocene and Palaeocene). In the area of the volcanic formations, a decreasing trend in vertical land motion is detected moving from Pleistocene and Oligo-Miocene deposits with peak values of -2.7 mm/yr (Fig. 9). The Palaeocene formations are characterised by the highest median and mean motion with respect to the Pliocene-Quaternary formations. The highest subsidence rates (i.e., -8.2 mm/yr) are detected in the Palaeocene formations located in the southern part of the study area, and localised subsidence may be correlated to local anthropogenic activities such as surface loading through new infrastructure and buildings.

The role of the structural setting of the study area was investigated by extracting profiles from the InSAR-derived estimates of vertical land motion across the tectonic fault (Fig. 10). Sections A–A' and B–B' reveal a certain agreement between discontinuities or peaks in VLM and the fault location (Fig. 10). For both profiles, slightly lower rates of vertical land motion are observed in the north-western part of the fault. For the C–C' profile, peaks of high subsidence are evident in correspondence with the faults, and a high gradient of subsidence change is evident along the profile. The relation between vertical land motion and tectonic faults is less clear for cross-sections D–D', E–E', and F–F', which is probably due to the kinematics of these faults. However, to further unravel the complexity of tectonics in that region requires investigations of horizontal displacements in addition to vertical movements.

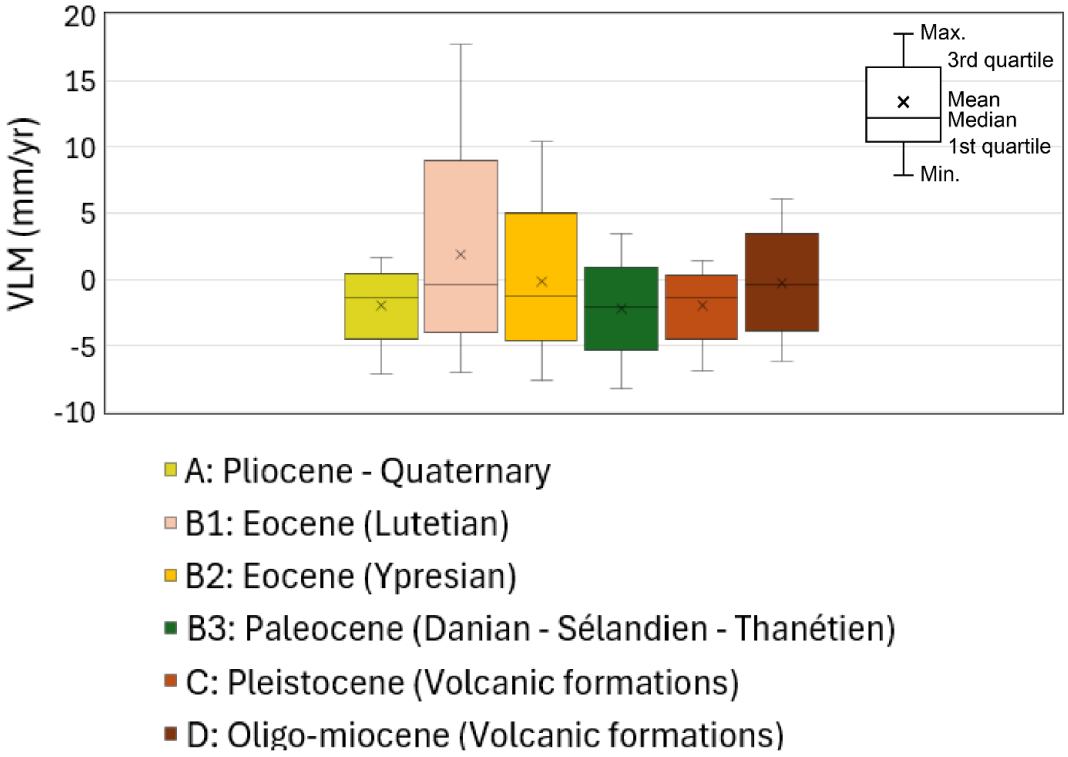

Figure 9 | Boxplot diagrams showing vertical land motion with relation to the age of geological units at the surface. Each boxplot shows the range between min. and max. values of vertical land motion (black bars), the range between 1st and 3rd quartiles (coloured bar), as well as median (black line in coloured bar) and mean (cross in coloured bar).

5.2 Relations between vertical land motion and hydrogeology and hydromechanics

Comparing the detected pattern of VLM with available information on hydrogeology and hydromechanics allows for insights whether aquifer characteristics and changes in groundwater level can be associated to the spatio-temporal pattern of vertical displacement. The comparison with hydrogeological units (Figs. 4 and 11) revealed that the highest average subsidence rates occur in the palaeo-valleys' clayey fill sand and the infrabasaltic sands. In particular, the average displacement rate in these units was approximately -2.7 mm/yr, indicating a moderate rate. Among these, the palaeo-valleys' clayey fill sand exhibited the highest peak of negative VLM, with rates reaching as much as -13.0 mm/yr. Furthermore, only the non-karstified sandy limestone record exhibited median VLM values lower than -2.0 mm/yr (Fig. 11).

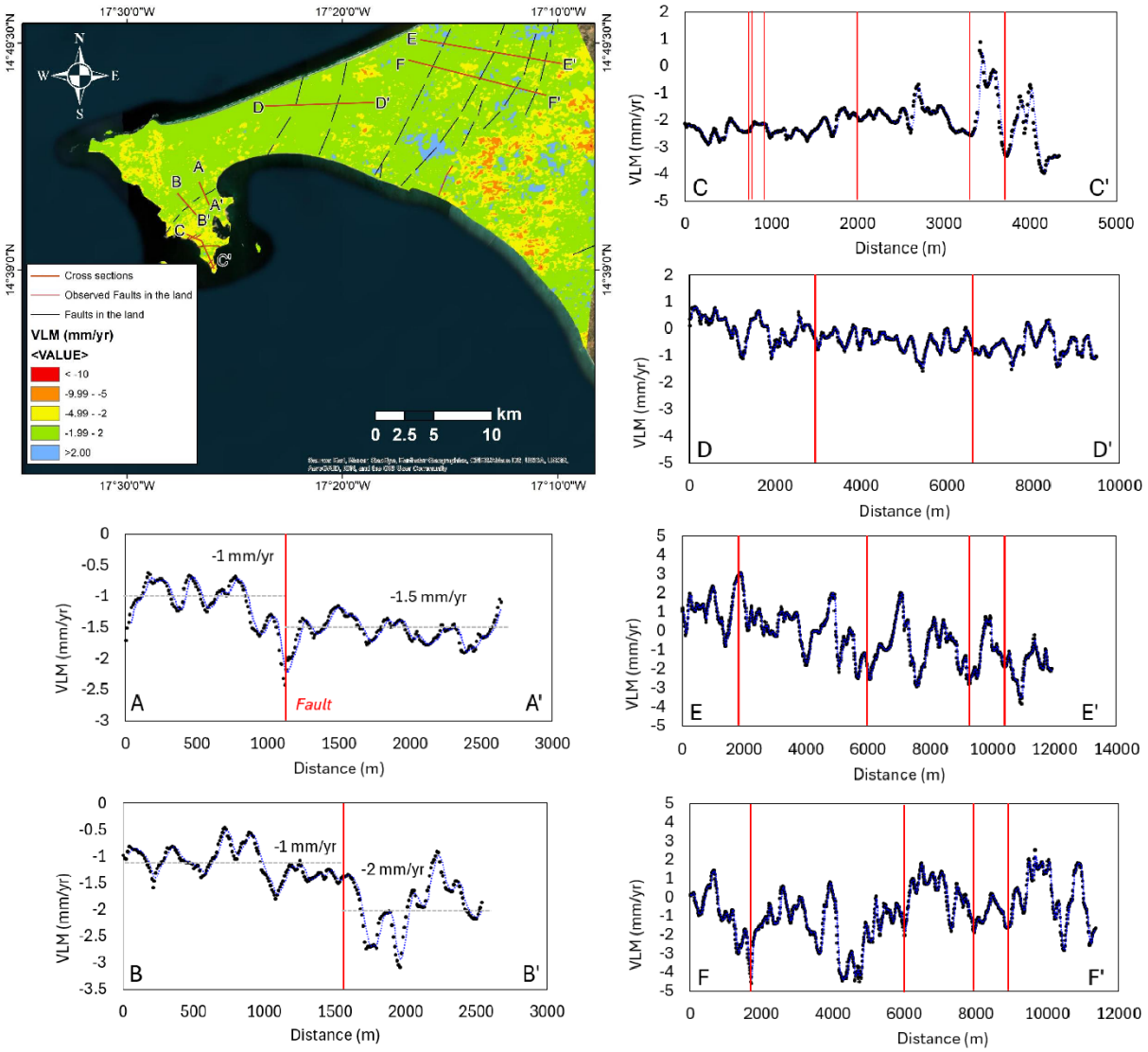

Figure 10 | Location of faults (i.e., observed and hypothesised faults) and profiles showing the spatial pattern of vertical land motion (VLM) (mm/yr) across tectonic faults.

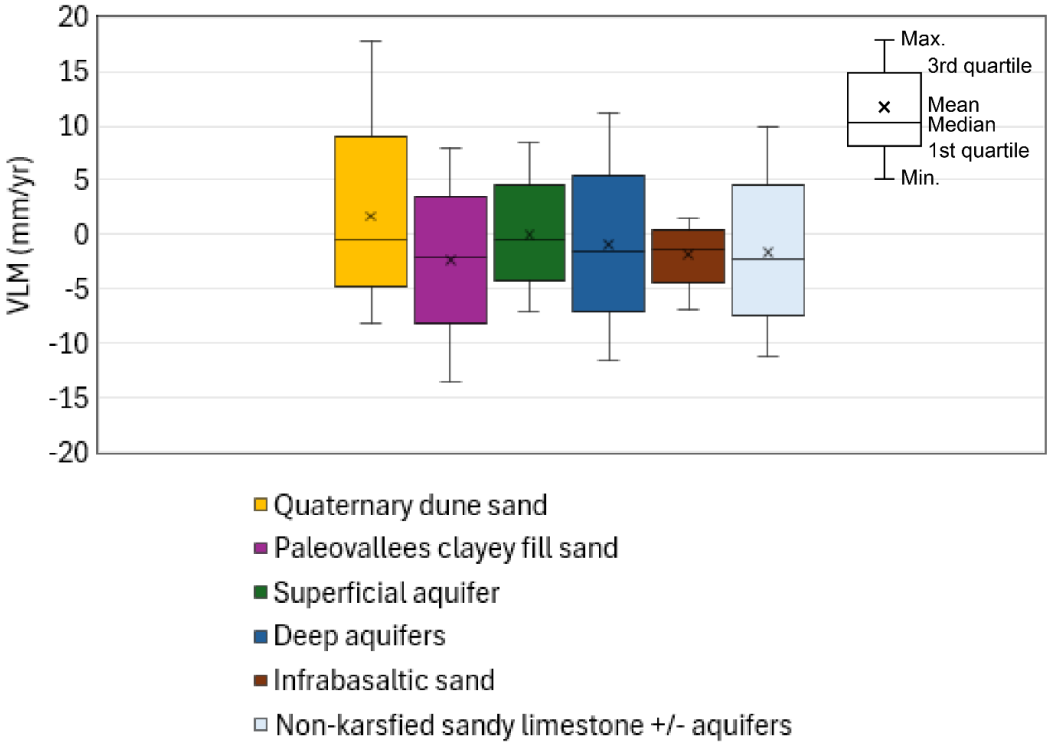

Figure 11 | Boxplot diagrams showing vertical land motion with relation to the hydrogeological units. Each boxplot shows the range between min. and max. values of vertical land motion (black bars), the range between 1st and 3rd quartiles (coloured bar), as well as median (black line in coloured bar) and mean (cross in coloured bar).

Comparing the InSAR derived VLM estimates with the observed groundwater level changes (see also Section 3.1) shows moderate subsidence rates along with groundwater level variations. To further investigate these relations, five buffer zones with a radius ranging from 100 m to 500 m were created around the three piezometers shown in Fig. 4. The average displacement rate was extracted within each buffer zone to evaluate any trends with increasing distance from the piezometers. The results show that, only in case of the piezometer Ouakam Cite Amar, which recorded a value of -16.6 m in 2023, values of approximately -2.5 mm/yr are observed near the piezometer. The VLM rate tends to decrease (i.e. less subsiding) with increasing distance, reaching values of around 2.0 mm/yr at greater distances (Fig. 12). For the other two piezometers, no clear trend could be detected (Fig. 12).

5.3 Relations between vertical land motion and land use

The statistical analysis of the vertical land motion in relation to land use/land cover classes revealed that high negative rates, exceeding -10 mm/yr, are evident across built-up areas, rangelands, and bare ground (Fig. 13). Cropland areas exhibit the highest median values of negative vertical displacement. This might be because groundwater is used to supply water for crop production. Fig. 14 shows a few examples of photos taken in the cropland areas through Google Street View in sites characterized by the largest subsidence rates (in the order of 5 to

10 mm/year). Evidence of boreholes and water supply system are clearly visible. Consequentially, aquifer compaction could be responsible for the measured VLM.

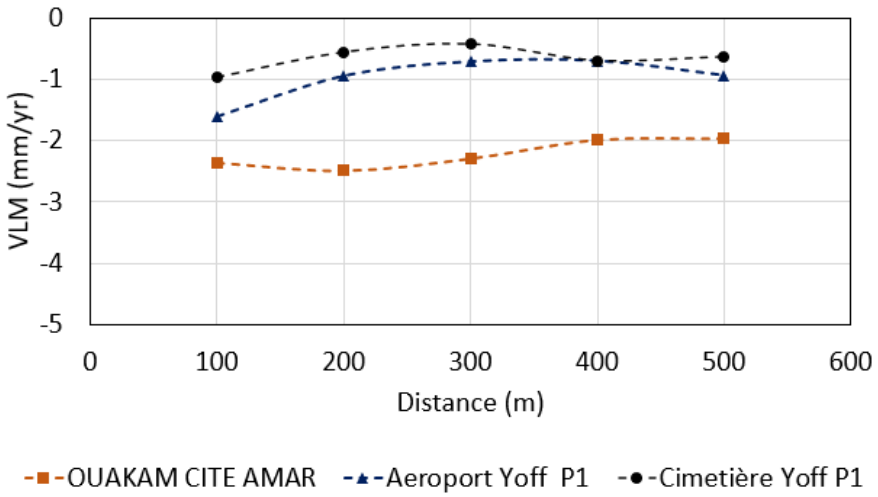

Figure 12 | Average vertical land motion with respect to distance from piezometers Ouakam Cite Amar, Aeroport Yoff P1 and Cimetière Yoff P1.

Focusing on the built-up environment, local hotspots of subsidence are located in the vicinity of Léopold Sédar Senghor International Airport, as well as in newly developed areas near the Mamelles seawater desalination plant in Dakar (Fig. 15). This evidence highlights the localised, moderate, and temporary ground displacement phenomena that are caused by human activities, particularly construction and infrastructural development.

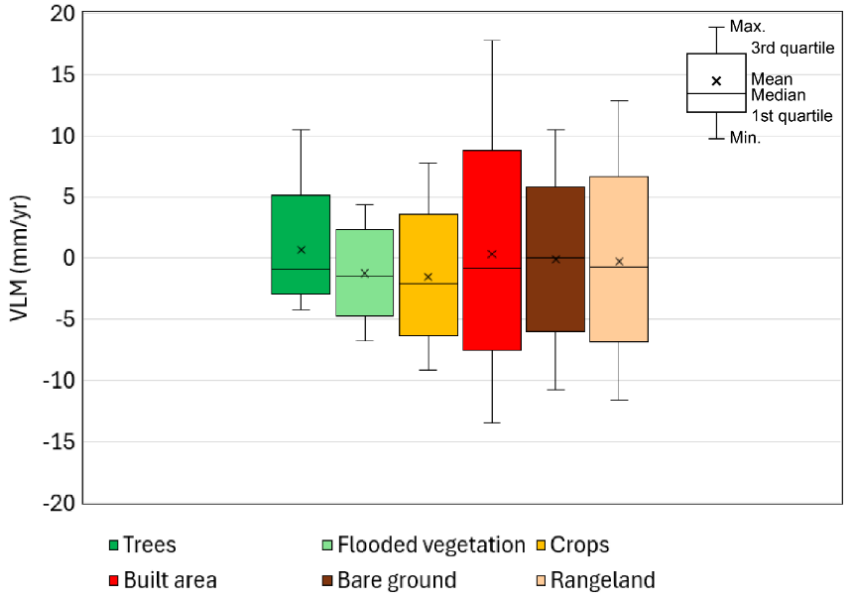

Figure 13 | Boxplot diagrams showing vertical land motion with relation to the land use/land cover classes. Each boxplot shows the range between min. and max. values of vertical land motion (black bars), the range between 1st and 3rd quartiles (coloured bar), as well as median (black line in coloured bar) and mean (cross in coloured bar).

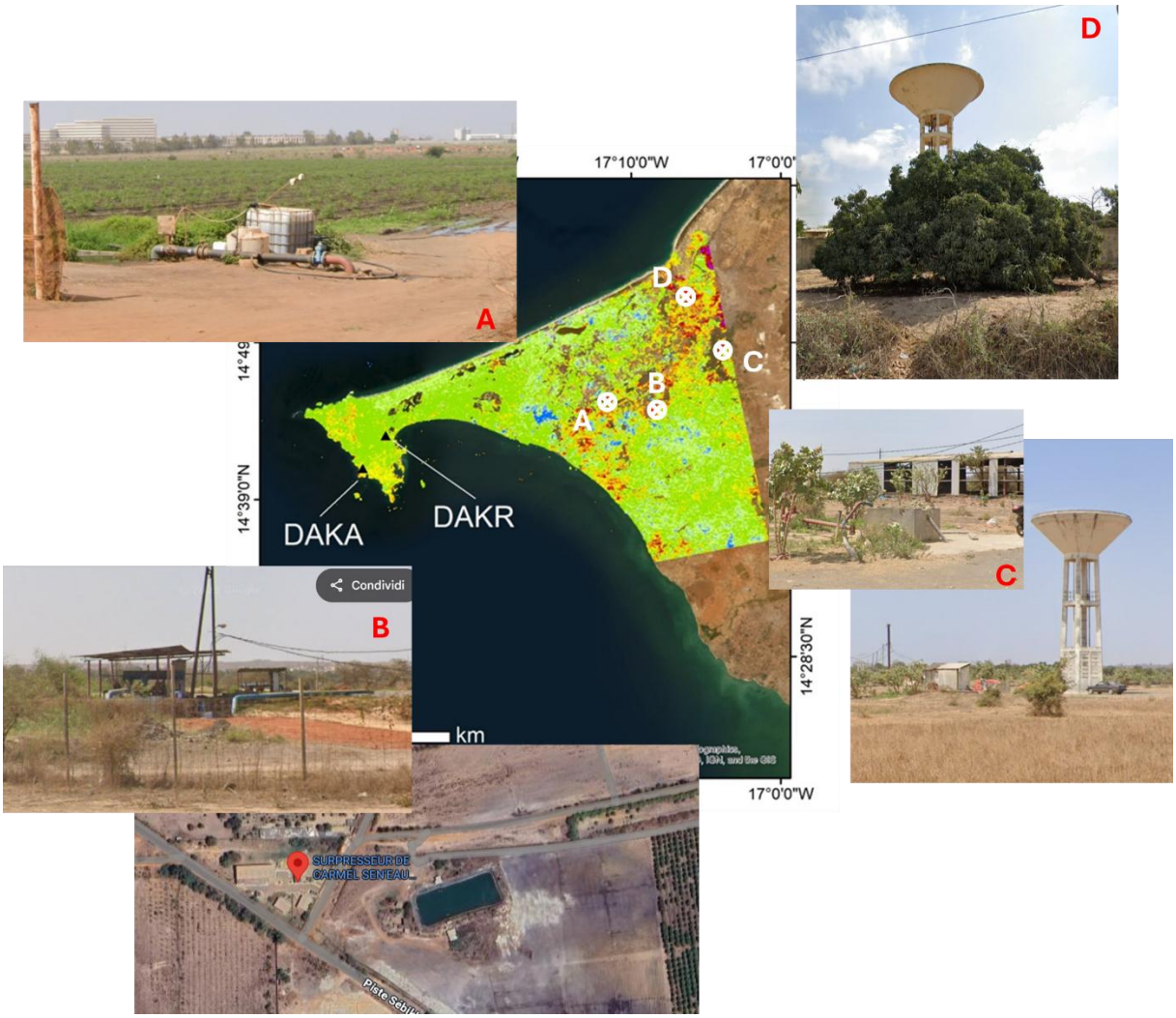

Figure 14 | Screenshots taken from Google Street View showing water distribution and storing systems in four locations (labelled A to D) characterized by a land subsidence rate from 5 to 10 mm/year. The sites are in cropland areas.

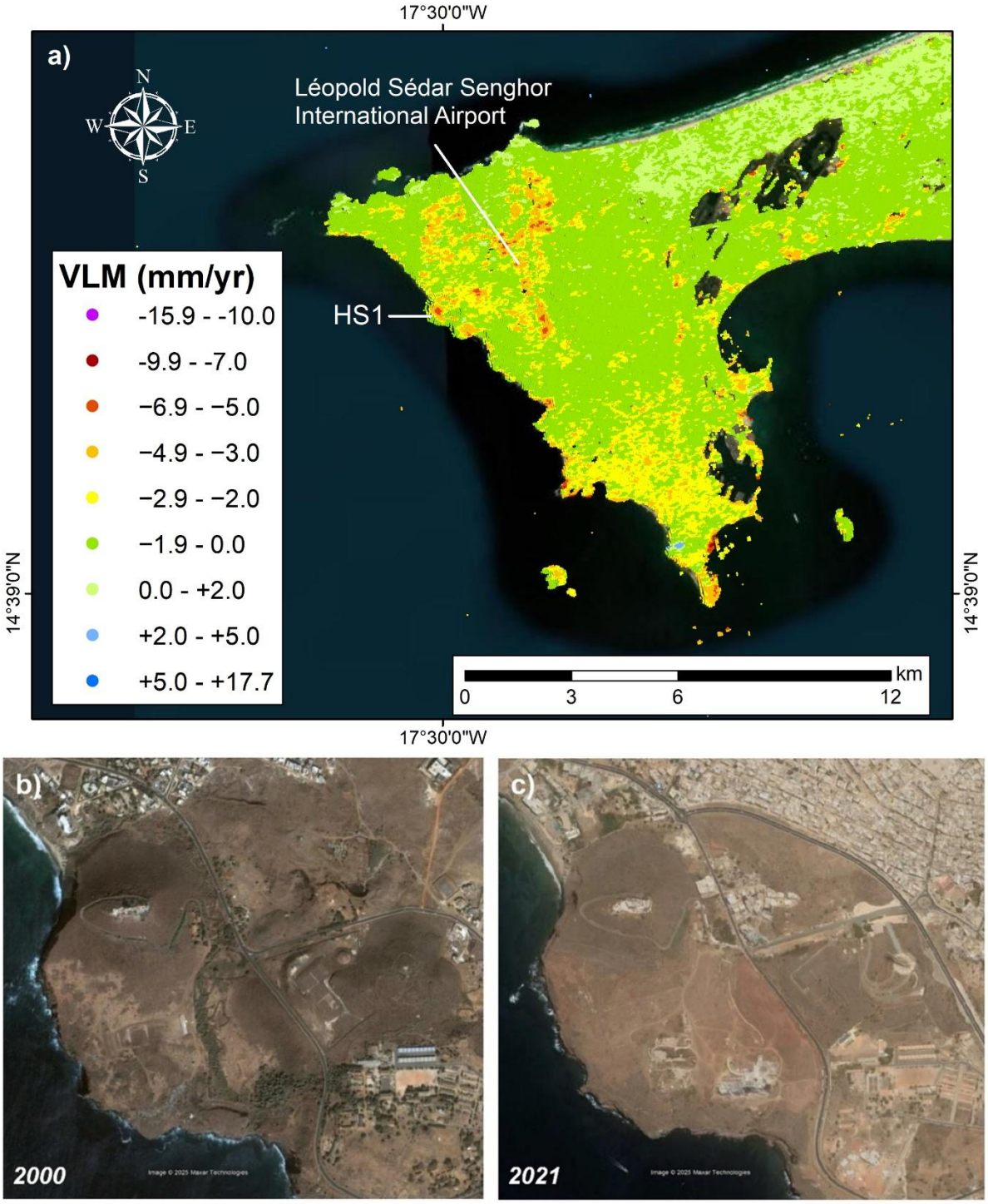

Figure 15 | Local hotspots of land subsidence in the Cape Verde Peninsula (a) and Google Earth imagery showing the expansion of built-up areas in the vicinity of the Mamelles seawater desalinisation plant (HS1 in (a)) in Dakar which occurred between 2000 (b) and 2021 (c). Source of background image in (a): Esri, Maxar, GeoEye, Earthstar Geographics, CNES/Airbus DS, USDA, USGS, AeroGRID, IGN, and the GIS User Community.

A further analysis has been performed to evaluate the role of human settlement evolution by using the World Settlement Footprint (WSF) Evolution dataset. This dataset provides a detailed overview of global settlement extents over time, utilising a high-resolution (i.e., 30 m) dataset that maps urban growth of settlement areas worldwide on an annual basis from 1985 to 2015 (Marconcini et al., 2020). The results indicate that the majority of the existing settlements were established prior to 1985, with significant new recent urban expansion primarily occurring along the coast (Fig. 16a). As these newly expanded areas are prone to relative sea-level rise, this coastal urbanisation trend highlights the increased exposure of the coastal population and any land-use, infrastructural and socio-economic assets.

Comparing rates of VLM for different construction periods reveals that the median values exhibit a gradual and rough increase from the buildings constructed around 1992 to the older (i.e., 1985), suggesting that older structures may be more susceptible to structural problems, possibly due to aging materials, and/or outdated construction standards. This increasing trend in median displacement values over time gives insight into the need for maintenance of older buildings. Conversely, for buildings constructed between 1998 and 2015, the observed increase in median displacement values might be attributed to ongoing consolidation. Notably, the highest median value is observed for buildings constructed in 2006, reaching approximately 2.9 mm/year (Fig. 16b).

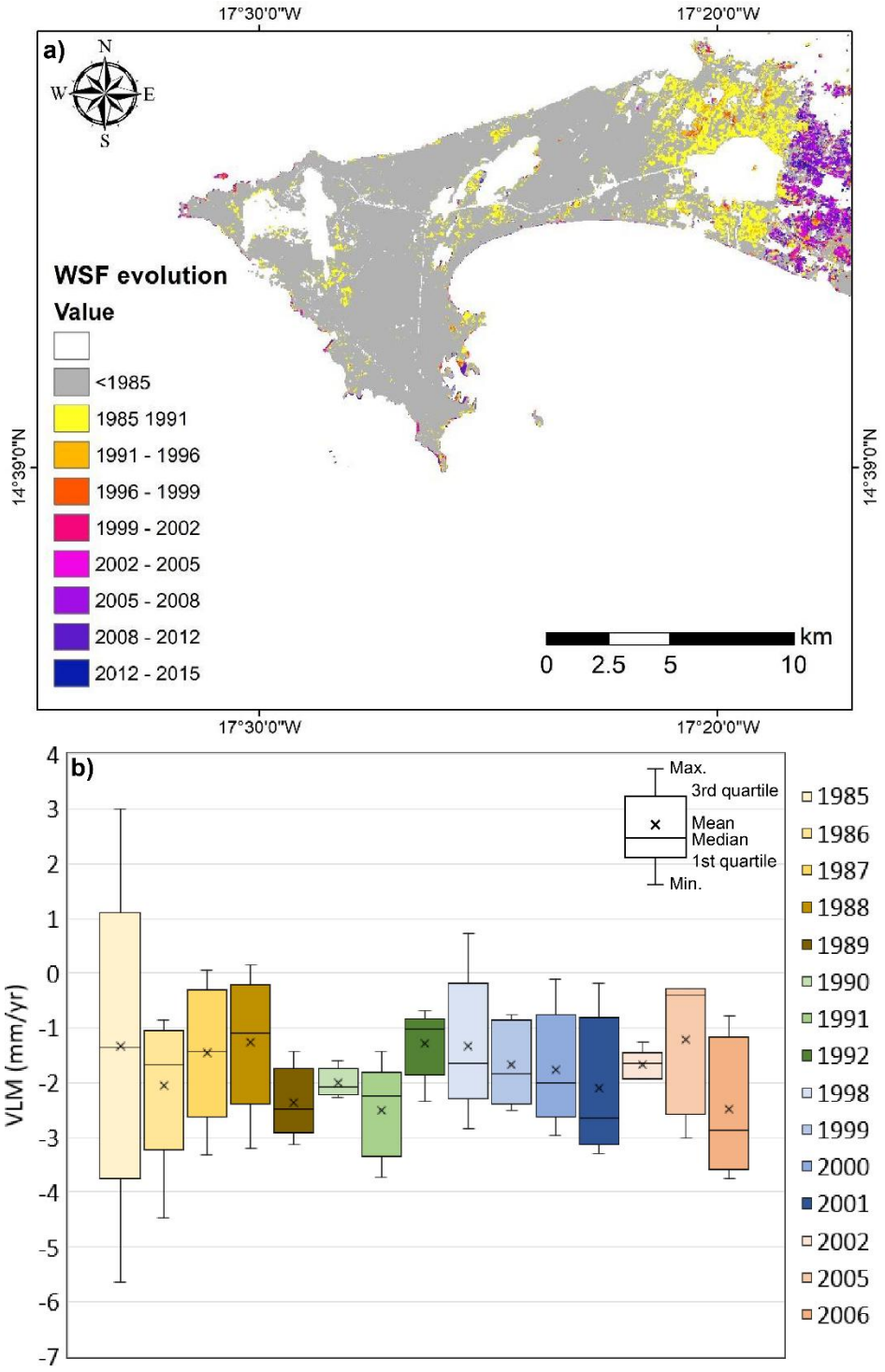

Figure 16 | World Settlement Footprint (WSF) evolution map from 1985 to 2015, showing settlement growth over time (a), and boxplot diagrams showing vertical land motion with relation to building age. Each boxplot shows the range between min. and max. values of vertical land motion (black bars), the range between 1st and 3rd quartiles (coloured bar), as well as median (black line in coloured bar) and mean (cross in coloured bar).

6 Implications for relative sea-level rise and flood exposure

In order to move from the assessment of vertical land motion towards thorough assessments of coastal exposure towards relative sea-level rise (and also flooding) requires adequate integration of rates of VLM and global sea-level rise with coastal land elevation that is properly aligned to sea level. Consequently, coastal elevation above sea level is one key determinant of exposure. As the integration of VLM, sea-level rise and coastal elevation is currently still work in progress, we here for now focus on land elevation and topography and refer to elevation information derived from one of the latest available global digital elevation model (DEM), i.e. DeltaDTM (Pronk et al., 2024) (Fig. 17).

The peninsula's topography is characterised by a relatively gentle slope ascending from the coastline inland, with elevations predominantly ranging between 0 and 50 m above sea level. Low-lying plains, which are particularly susceptible to sea-level rise and coastal erosion, are evident in the northern part of the harbour as well as in the north of the peninsula (Fig. 17). Moving inland, the terrain gradually elevates, reaching higher elevations of approximately 50 to 96 m in the northwestern parts of the city. As the majority of the coastal lowland is higher than 1 m above sea level, the exposure to 1 m relative sea-level rise is comparably less than observed for other regions along the Gulf of Guinea. However, as vast parts of the peninsula are within the low-elevation coastal zone, i.e., ≤10 m above sea level, points to the potential risk of these areas towards other coastal hazards such as coastal flooding.

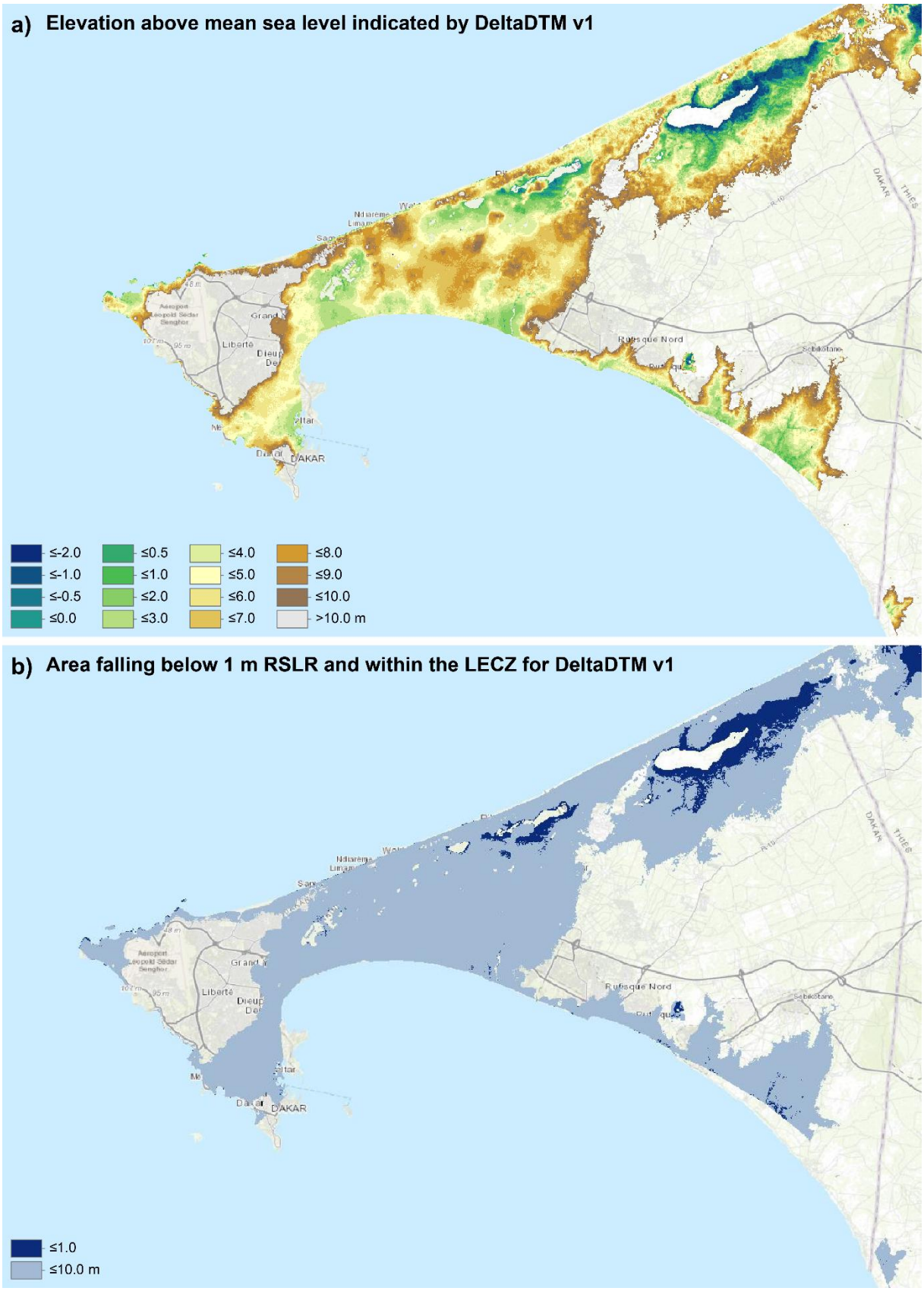

Figure 17 | Elevation map of Dakar based on DeltaDTM v1, vertically referenced to actual, continuous local mean sea level as indicated by latest available mean dynamic topography (Jousset et al., 2023) (a), and area falling below 1 m RSLR and within the LECZ- Low Elevation Coastal Zone (b).

7 Conclusions and outlook

Land subsidence in the Dakar Port region is a multi-factorial phenomenon rooted in geological, hydrological, and anthropogenic dynamics and their interaction. Based on new, InSAR-derived estimates of vertical land motion, which were processed under the umbrella of the ENGULF program, rates of land subsidence are comparably moderate. On local scale, these rates seem to be primarily driven by human activities, notably urban development around the international airport and the harbour, thereby confirming previous studies in the port area. The larger pattern of moderate vertical land motion in the southern parts of Dakar is likely controlled by the regional tectonic setting while the lithostratigraphy seems sensitive to chemical and mechanical degradation, leading to a potential increase in compaction susceptibility in the future if marine intrusion and increasing loading continue. Although Dakar is one of Africa's most populous urban centres (World Population Review, 2025), groundwater exploitation does not appear to significantly contribute to land subsidence. This is likely due to the geological characteristics of the subsurface, specifically the relatively small thickness of compressible Quaternary deposits, which are generally the most susceptible to compaction, as well as the poor quality of groundwater used for potable purposes, which discourages excessive extraction (Re et al., 2011). It should be noted that geomechanical characterization of the various deposits is completely lacking. Analysing vertical land motion over time by comparison with periods of land use/land cover and construction highlights the increased exposure of the coastal population as well as land-use, infrastructural and socio-economic assets. Though the Cape Verde Peninsula seems to be less exposed to relative sea-level rise of up to 1 m, further targeted in-situ investigations are needed to mitigate and prevent (future) land subsidence that may enhance relative sea-level rise, especially in the urban areas of Dakar which are projected to increase in the future (World Population Review, 2025). As vast parts of the peninsula are less than 10 m above sea level and therefore prone also to other coastal hazards and impacts such as flooding and erosion, coastal exposure and vulnerability assessments and adaptation and mitigation strategies are required to be inclusive, addressing the broad range of coastal hazards and factors in the region.

Despite limited available data, this study suggests that groundwater pumping-induced land subsidence may now be more significant inland within the Cape Verde Peninsula than in Dakar. Land subsidence rates of up to 10 mm/year have been observed in croplands established above deep and Quaternary dune aquifers. Evidence of groundwater use has been gathered from online sources. These areas are situated at altitudes above 10 meters above sea level, mitigating the risk of increased flooding despite high subsidence rates. However, the subsidence may still pose threats to infrastructure functioning and stability. It is important to

note that these conclusions are drawn from limited data and would benefit from further investigation.

The general region's low susceptibility to anthropogenic land subsidence is primarily due to the absence of thick, highly compressible deposits. However, to strengthen resilience in the study area, the following actions are recommended to improve the knowledge on land subsidence and relative sea-level rise in the region and provide fundamental information for risk adaptation and mitigation:

- Implement a comprehensive, continuous monitoring system across the region to track vertical and horizontal ground displacements, groundwater levels, and structural health of infrastructure.
- Establish a permanent piezometric monitoring network near sensitive zones (Km5, Hann, Port basin) to track real-time aquifer behaviour.
- Deploy GNSS stations to ground-truth InSAR-derived spatio-temporal estimates of vertical land motion.
- Regulate and monitor groundwater abstraction, particularly from confined aquifers, by enforcing sustainable quotas.
- Promote artificial recharge strategies, including stormwater infiltration zones or treated wastewater injection.
- Promote sustainable urban planning of the coastal areas that incorporates vertical land motion hazard mapping and vulnerability assessments.
- Update urban planning regulations to reflect subsidence risk maps, especially before any port expansion.
- Conduct detailed geotechnical and geomechanical surveys prior to major construction to assess compaction risks.
- Monitor hydrochemical evolution, focusing on salinity indicators (Na^+, Cl^-, SO_4^{2-}) to evaluate ongoing marine influence.
- Integrate multidisciplinary data (geophysics, drilling logs, water chemistry, structural geology) for a dynamic vulnerability model of the region.

References

Almar, R., Stieglitz, T., Addo, K. A., Ba, K., Ondoa, G. A., Bergsma, E. W., Bonou, F., Dada, O., Angnuureng, D., & Arino, O. (2023). Coastal zone changes in West Africa: challenges and opportunities for satellite earth observations. *Surveys in Geophysics*, *44*(1), 249–275. https://doi.org/10.1007/s10712-022-09721-4.

Alves, B., Angnuureng, D. B., Morand, P., & Almar, R. (2020). A review on coastal erosion and flooding risks and best management practices in West Africa: what has been done and should be done. *Journal of Coastal Conservation*, *24*(3), 38. https://doi.org/10.1007/s11852-020-00755-7.

Ankrah, J., Monteiro, A., & Madureira, H. (2023). Shoreline change and coastal erosion in West Africa: A systematic review of research progress and policy recommendation. *Geosciences*, *13*(2), 59. https://doi.org/10.3390/geosciences13020059.

Barusseau, J. P., Duvail, C., Noel, B. J., Nehlig, P., Roger, J., & Serrano, O. (2009). *Notice explicative de la carte géologique du Sénégal à 1/500 000, feuilles nord-ouest, nord-est et sud-ouest*.

British Geological Survey. (2023). *Geology of Senegal*. Africa Groundwater Atlas. Consulté sur : https://en.wikipedia.org/wiki/Geology_of_Senegal

Dada, O., Almar, R., Morand, P., & Menard, F. (2021). Towards West African coastal social-ecosystems sustainability: Interdisciplinary approaches. *Ocean & Coastal Management*, *211*, 105746. https://doi.org/10.1016/j.ocecoaman.2021.105746.

Dada, O. A., Almar, R., & Morand, P. (2024). Coastal vulnerability assessment of the West African coast to flooding and erosion. *Scientific Reports*, *14*(1), 890. https://doi.org/10.1038/s41598-023-48612-5.

Esri and Impact Observatory (2025). Esri Sentinel-2 10m Land Use/Land Cover. https://livingatlas.arcgis.com/landcover/, last access: 2025-07-22.

Faye, S., Ndour, N., & Fall, M. (2019, January). Isotopic evidence of the deep Maastrichtien aquifer in the Senegal. In *46th Annual Congress of the International Association of Hydrogeologists* (pp. 193-193).

Hanssen, R.F. (2001). *Radar interferometry, data interpretation and error analysis*. Kluwer Academic Publishers

Jousset, S., Mulet, S., Greiner, E., Wilkin, J., Vidar, L., Dibarboure, G., & Picot, N. (2023). New Global Mean Dynamic Topography CNES-CLS-22 Combining Drifters,

Hydrological Profiles and High Frequency Radar Data. *ESS Open Archive*. https://doi.org/10.22541/essoar.170158328.85804859/v2.

Kane, C. H., Diene, M., Fall, M., Sarr, B., & Thiam, A. (2012). Reassessment of the resources of a deep aquifer system under physical and chemical constraints: the maastrichtian aquifer. *Journal of Water Resource and Protection*, *4*(4), 217-223.

Le Cozannet, G., Raucoules, D., Wöppelmann, G., Garcin, M., Da Sylva, S., Meyssignac, B., Gravelle, M., & Lavigne, F. (2015). Vertical ground motion and historical sea-level records in Dakar (Senegal). *Environmental Research Letters*, *10*(8), 084016. https://doi.org/10.1088/1748-9326/10/8/084016.

Lee, J. C., & Shirzaei, M. (2023). Novel algorithms for pair and pixel selection and atmospheric error correction in multitemporal InSAR. *Remote Sensing of Environment*, *286*, 113447. https://doi.org/10.1016/j.rse.2022.113447.

Marconcini, M., Metz-Marconcini, A., Üreyen, S., Palacios-Lopez, D., Hanke, W., Bachofer, F., Zeidler, J., Esch, T., Gorelick, N., Kakarla, A., Paganini, M., & Strano, E. (2020). Outlining where humans live, the World Settlement Footprint 2015. *Scientific Data*, *7*(1), 242. https://doi.org/10.1038/s41597-020-00580-5.

Pronk, M., Hooijer, A., Eilander, D., Haag, A., de Jong, T., Vousdoukas, M., Vernimmen, R., Ledoux, H., & Eleveld, M. (2024). DeltaDTM: A global coastal digital terrain model. *Scientific Data*, *11*(1), 273. https://doi.org/10.1038/s41597-024-03091-9.

Re, V., Cissé Faye, S., Faye, A., Faye, S., Gaye, C. B., Sacchi, E., & Zuppi, G. M. (2011). Water quality decline in coastal aquifers under anthropic pressure: the case of a suburban area of Dakar (Senegal). *Environ. Monit. Assess.*, *172*, 605–622. https://doi.org/10.1007/s10661-010-1359-x.

Roger, J., Banton, O., Barusseau, J. P., Castaigne, P., Comte, J. C., Duvail, C., Nehlig, P., Noel, B., Serrano, O., & Travi, Y. (2009). *Notice explicative de la cartographie multi-couches à 1/50,000 et 1/20,000 de la zone d'activité du Cap-Vert, Sénégal*.

Shirzaei, M., & Bürgmann, R. (2012). Topography correlated atmospheric delay correction in radar interferometry using wavelet transforms. *Geophysical Research Letters*, *39*(1), L01305. https://doi.org/10.1029/2011GL049971.

Shirzaei, M. (2013). A wavelet-based multitemporal DInSAR algorithm for monitoring ground surface motion. *IEEE Geoscience and Remote Sensing Letters*, *10*(3), 456–460. https://doi.org/10.1109/LGRS.2012.2208935.

Shirzaei, M., Manga, M., & Zhai, G. (2019). Hydraulic properties of injection formations constrained by surface deformation. *Earth and Planetary Science Letters*, *515*, 125–134. https://doi.org/10.1016/j.epsl.2019.03.025.

Spengler, A., Castelain, J., & Cauvin, J. (1966). Le bassin secondaire-tertiaire du Sénégal. In *Symposium/Bassins sédimentaires côtiers Post-Cambrien de l'Ouest de l'Afrique* (pp. 80–94).

World Population Review (2025). Dakar. https://worldpopulationreview.com/cities/senegal/dakar, last access: 2025-07-23.